Title

Brain and behaviour phenotyping of a mouse model of neurofibromatosis type-1: an MRI/DTI study on social cognition

Journal

Genes Brain & Behavior, 15(7)

ISSN

1601-1848

Authors

Petrella, LI
Cai, Y
Sereno, JV
et al.

Publication Date

2016-09-01

DOI

10.1111/gbb.12305

Peer reviewed

HHS Public Access

Author manuscript

Genes Brain Behav. Author manuscript; available in PMC 2017 September 19.

Published in final edited form as:

Genes Brain Behav. 2016 September ; 15(7): 637–646. doi:10.1111/gbb.12305.

Brain and behaviour phenotyping of a mouse model of neurofibromatosis type-1: an MRI/DTI study on social cognition

L. I. Petrella[†,‡], **Y. Cai**[§,¶,**,††,‡‡], **J. V. Sereno**[†,‡], **S. I. Gonçalves**[†,‡], **A. J. Silva**[§,¶,**,††,‡‡], and **M. Castelo-Branco**[†,‡,*]

[†]Institute of Nuclear Science Applied to Health, University of Coimbra, Coimbra, Portugal

[‡]Center for Neuroscience and Cell Biology - Institute of Biomedical Imaging and Life Science (CNCIBILI), University of Coimbra, Coimbra, Portugal

[§]Department of Neurobiology, University of California, Los Angeles, CA, USA

[¶]Department of Psychology, University of California, Los Angeles, CA, USA

[**]Department of Psychiatry and Biobehavioral Sciences, University of California, Los Angeles, CA, USA

[††]Integrative Center for Learning and Memory, University of California, Los Angeles, CA, USA

[‡‡]Brain Research Institute, University of California, Los Angeles, CA, USA

Abstract

Neurofibromatosis type-1 (NF1) is a common neurogenetic disorder and an important cause of intellectual disability. Brain-behaviour associations can be examined *in vivo* using morphometric magnetic resonance imaging (MRI) and diffusion tensor imaging (DTI) to study brain structure. Here, we studied structural and behavioural phenotypes in heterozygous Nf1 mice ($Nf1^{+/-}$) using T2-weighted imaging MRI and DTI, with a focus on social recognition deficits. We found that $Nf1^{+/-}$ mice have larger volumes than wild-type (WT) mice in regions of interest involved in social cognition, the prefrontal cortex (PFC) and the caudate-putamen (CPu). Higher diffusivity was found across a distributed network of cortical and subcortical brain regions, within and beyond these regions. Significant differences were observed for the social recognition test. Most importantly, significant structure–function correlations were identified concerning social recognition performance and PFC volumes in $Nf1^{+/-}$ mice. Analyses of spatial learning corroborated the previously known deficits in the mutant mice, as corroborated by platform crossings, training quadrant time and average proximity measures. Moreover, linear discriminant analysis of spatial performance identified 2 separate sub-groups in $Nf1^{+/-}$ mice. A significant correlation between quadrant time and CPu volumes was found specifically for the sub-group of $Nf1^{+/-}$ mice with lower spatial learning performance, suggesting additional evidence for

[*]Corresponding author: M. Castelo-Branco, Center for Neuroscience and Cell Biology - Institute of Biomedical Imaging and Life Science (CNC.IBILI), University of Coimbra, Azinhaga de Santa Comba, 3000-548, Coimbra, Portugal. mcbranco@fmed.uc.pt.

No conflicts of interests are to be reported by any of the authors.

Supporting Information: Additional supporting information may be found in the online version of this article at the publisher's web-site

reorganization of this region. We found strong evidence that social and spatial cognition deficits can be associated with PFC/CPu structural changes and reorganization in NF1.

Keywords

Brain; magnetic resonance imaging; mice; neurofibromatosis type-1; social cognition; spatial learning

Neurofibromatosis type-1 (NF1) is a relatively frequent neurogenetic disorder with a prevalence of 1/3500 worldwide. Mutations in the NF1 gene lead to loss of function of neurofibromin which is a negative regulator of cellular proliferation and differentiation (Theos & Korf 2006). Its role on synaptic plasticity, learning and memory is also well documented (Costa & Silva 2003; Shilyansky *et al.* 2010a, b).

Intellectual disabilities occur in up to 50% of NF1 children; they may manifest as cognitive slowing, memory disturbances, difficulties in solving strategic problems, visuospatial impairments, deficits in motor coordination, mental flexibility and affective disorders (Diggs-Andrews & Gutmann 2013; Ribeiro *et al.* 2012; Silva *et al.* 1997; Violante *et al.* 2013; Zöller *et al.* 1997). Recent evidence suggests that social cognitive deficits are common in NF1 and that this condition qualifies as an autism spectrum disorder (Lehtonen *et al.* 2013; Loitfelder *et al.* 2015; Plasschaert *et al.* 2015; Pride *et al.* 2013, 2014; Walsh *et al.* 2013).

As in NF1 subjects, behavioural studies in mouse models of NF1 have identified spatial learning (Shilyansky *et al.* 2010a,b) and motor coordination (van der Vaart *et al.* 2011) deficits. Studies with NF1 mouse models showed that increased Ras/MAPK (mitogen-activated protein kinases) signalling result in higher GABA (gamma-aminobutyric acid) release during learning and consequently in deficits in hippocampal long-term potentiation (LTP) that could account for the spatial learning and memory deficits of these mutant mice (Costa *et al.* 2002; Cui *et al.* 2008). Interestingly, treatment with lovastatin reversed the molecular, electrophysiological and learning deficits of these mice. Transcranial magnetic stimulation studies in NF1 patients also identified cortical potentiation deficits that seemed to be caused by enhanced inhibition and that could be reversed by treatment with lovastatin (Mainberger *et al.* 2013).

Shilyansky *et al.* (2010a,b) identified similar working memory deficits in $Nf1^{+/-}$ mice that resemble the human phenotype. In mice, the working memory deficits seemed to be caused by increased GABA neurotransmission in prefrontal cortex (PFC) and striatum. Human studies revealed working memory deficits, and functional magnetic resonance imaging (fMRI) studies indicated that these deficits were correlated with hypoactivation of PFC circuits, a result consistent with the idea that enhanced inhibition accounts for working memory deficits in NF1.

In parallel with studies that identified social cognition deficits in NF1 (Lehtonen *et al.* 2013; Plasschaert *et al.* 2015; Pride *et al.* 2013, 2014; Walsh *et al.* 2013), selective social learning deficits have also been identified in mice heterozygous for the Nf1 gene ($Nf1^{+/-}$), and

related to changes in GABA neurotransmission (Molosh *et al.* 2014). Consistent with previous electrophysiological findings in the hippocampus (Costa *et al.* 2002; Cui *et al.* 2008), studies in the amygdala have indeed suggested that social cognition deficits in $Nf1^{+/-}$ mice are caused by enhanced GABA neuro-transmission that lead to deficits in LTP (Molosh *et al.* 2014). Deletion of the p21 protein-activated kinase (Pak1) gene reversed the amygdala molecular and electrophysiological deficits and rescued the social learning deficits of these mice (Molosh *et al.* 2014). However, these therapeutic approaches may only reverse functional deficits and not the structural changes induced by abnormal cell proliferation during development.

Other studies revealed that phenotypic changes are not confined to neurons and identified mild astrocytic abnormalities in $Nf1^{+/-}$ mice. Rizvi *et al.* (1999) observed an increased number of astrocytes in periaqueductal grey (PAG) and nucleus accumbens (Acc) of $Nf1^{+/-}$ mice, as well as increased astrocyte sizes in PAG. Gutmann *et al.* (2001) showed that astrocytes from $Nf1^{+/-}$ mice have reduced cell attachment, actin cytoskeletal abnormalities as well as increased cell motility.

Structural brain abnormalities have been documented in NF1 patients, although their relation to learning and social cognition deficits remains elusive. Increases in the volume of cortical and subcortical structures have been frequently observed and are summarized in Table 1 (Balestri *et al.* 2003; Cutting *et al.* 2000; Duarte *et al.* 2014; Greenwood *et al.* 2005; Margariti *et al.* 2007; Moore *et al.* 2000; Pride *et al.* 2014; Steen *et al.* 2001). Magnetic resonance imaging (MRI) and diffusion tensor imaging (DTI) studies pointed to a generalized change in mean diffusivity (MD) associated with volumetric changes (for a summary see also Table 1) (Filippi *et al.* 2013; Karlsgodt *et al.* 2012; Santos 2011; Wignall *et al.* 2010; Zamboni *et al.* 2007).

It has been difficult to relate these structural findings with the cognitive impairments observed in NF1. Accordingly, the relation of grey matter (GM) changes with attention or social-cognitive deficits remains controversial (Cutting *et al.* 2002; Greenwood *et al.* 2005; Moore *et al.* 2000; Pride *et al.* 2014).

Although some studies of Nf1 mice models have been conducted using MRI, they were focused just on high-intensity lesions in T2-weighted images (Robinson *et al.* 2010; Rosenbaum *et al.* 1999). Brain studies comparing MRI findings in Nf1 mouse models and NF1 subjects would be invaluable in validating these models. Additionally, structural deficits might emerge as key biomarkers for clinical investigation, and these deficits can also be studied in mouse models. In this study, we addressed brain morphometry in $Nf1^{+/-}$ mice, in key regions involved in social cognition, using T2-MRI as well as DTI, as well as the relation between the structural phenotypes of these mice and social cognition deficits.

Materials and methods

Mice models

$Nf1^{+/-}$ mice were F1 hybrids from a cross between C57BL/6NTac and 129T2/SvEmsJ. All experiments used littermates as controls and were done with the experimenter blinded to

genotype. A total number of 13 wild-type (WT, 4 males and 9 females) and 15 $Nf1^{+/-}$ (8 males and 7 females) mice were randomly chosen for behavioural assessment and MRI/DTI studies (due to technical reasons, 1 $Nf1^{+/-}$ mouse and 4 WT mice were excluded from the structural studies). Animals were group housed (2–4) on a 12h light/dark cycle in vivarium at University of California Los Angeles (UCLA), CAU and CNC.IBILI. All included animals were healthy (discomfort score 0). Experimenters were blind for genotype. All mice completed successfully the behavioural component of this study at UCLA, USA, and were then transported to the University of Coimbra, Portugal, for structural studies.

All efforts were made to reduce animal stress along the experimental stages and transportation, and both groups were submitted exactly to the same procedure to minimize group effect. The phenotype for the animal model is stable up to 10 months of age, and all the measurements were comprised between this period: behavioura tests between 3 and 5 months of age and MRI/DTI acquisitions between 6 and 8 months of age.

All experimental protocols at the UCLA were approved by the Chancellor's Animal Research Committee of the University of California, Los Angeles, in accordance with National Institutes of Health (NIH) guidelines. At the University of Coimbra, animal experiments were conducted according to the European Council Directives on Anima Care (2010/63/UE) and to the National Authorities

MRI acquisition

In vivo image acquisitions were conducted with a 9.4T magnetic resonance small animal scanner (BioSpec 94/20, Bruker Corporation, Ettlingen, Germany), at the Institute for Nuclear Sciences Applied to Health (ICNAS), University of Coimbra. Animals were anesthetised with isoflurane (delivered through the system E-Z SA800, Euthanex, Palmer, PA, USA), with constant temperature monitoring (Haake SC 100, Thermo Scientific, Waltham, Massachusetts, USA) and assessment of cardiorespiratory function (1030, SA Instruments Inc., Stony Brook, NY, USA).

For volumetric analyses, T2-weighted images were acquired in coronal planes using a RARE sequence: repetition time (TR) = 3800 ms; echo time (TE) = 33 ms; 10 averages; pixel size of 0.0781 mm × 0.0781 mm and slice thickness of 0.5 mm without spacing between slices (total head 256 pixels × 256 pixels × 34 slices)

For diffusivity analyses, DTI images were acquired using an EPI (echo-planar imaging) sequence with 85 gradient directions; b-value = 1000 second/mm^2; TR = 3000 milliseconds; TE = 18.5121 milliseconds; pixel size = 0.1563 mm × 0.1563 mm and slice thickness = 0.5 mm, without spacing between slices (total head 128 pixels × 128 pixels × 21 slices).

Volumetric analysis

For the analyses of brain structure volumes, images were pre-processed and segmented in Matlab R2012b, version number 8, including the following steps. (1) Correction of magnetic field inhomogeneity generated from the surface coil: the corrections were implemented using intensity curves from T2-weighted images obtained for an homogeneous phantom, and acquired with the same coil and system configuration. (2) Images were co-reregistered to the

same space of a reference volume using rigid transformation (this reference was created from the mean of seven co-registered brain volumes, apart from this study). (3) The heads were skull-stripped using a binary mask. (4) Brain intensities were normalized to match the range of a custom made template. (5) Images were segmented (labelled) into 27 structures following the Markov Random Field approach (Fischl *et al.* 2002), and using a custom made template. (6) After automatic segmentation, manual corrections were performed in the structures of interest (i.e. PFC, caudate putamen -CPu- and the hippocampus) to further minimize potential errors resulting from the procedure inaccuracies. We implemented this procedure in Matlab, where the T2-weighted image and the corresponding segmentation are superimposed, and after visual inspection, the operator redefines the misaligned borders of the structures of interest using a cursor (7) The volume values were computed by multiplying the number of voxels labelled as belonging to each structure of interest, by the voxel size. An example of the images resulting from the T2-weighted sequence and the resulting segmentation is presented in Fig. 1. (8) Independent samples *t*-tests were implemented for each structure, to depict the existence of significant differences between volumes of WT and $Nf1^{+/-}$ mice (significance level = 5%). (9) The testing of a gender effect in the measured volumes was performed using analysis of variance (anova).

DTI analysis

We analysed fractional anisotropy (FA), radial diffusivity (RD) and the $\lambda 1$ diffusion tensor eigenvalue, involving the following steps. (1) Eddy current correction was applied using the FDT diffusion toolbox of the FMRIB's Software Library (FSL). (2) Using the same software and toolbox, parametric maps were constructed, including images with inactive diffusion gradient (b0), MD, FA, $\lambda 1$, $\lambda 2$ and $\lambda 3$ maps (see Figure S1, Supporting Information, for representative data). (3) Using the b0 maps, images from each mouse were co-registered to the same space. First, b0 images from WT mice were co-registered with the b0 map of one mouse; next, we computed the mean from b0 maps of all WT mice; finally, the b0 maps from all WT and $Nf1^{+/-}$ mice were co-registered to the mean-b0 map, and the resultant transformation matrix was applied to the remaining parametric maps. In this step, an affine transformation with nine parameters was applied, using Matlab R2012b. (4) The RD maps for each mouse were constructed as $(\lambda 2+ \lambda 3)/2$. (5) The maps were smoothed using the Statistical Parametric Mapping, version number 8 (SPM8) software, with an isotropic Gaussian kernel, FWHM (full width to half maximum) [mm] =[0.5 0.5 0.5]. (6) Statistical analyses for comparison between WT and $Nf1^{+/-}$ characteristics were first performed through independent samples Student's *t*-tests in a voxel-by-voxel wise.

The significance level was set at $P = 5\%$ followed by false discovery rate (FDR) correction for multiple comparisons ($Q = 5\%$). (7) Also, the averages of diffusivity parameters were computed over the structures of interest using binary masks, and analysed by independent samples Student's *t*-tests (significance level = 5%).

Behavioural assessment

Morris water maze—In the hidden-platform version of the Morris water maze, mice were trained with two trials per day for five consecutive days [inter-trial interval (ITI) = 1 min]. This training regimen is ideal to not over train the mice, and better detect a difference

between $Nf1^{+/-}$ and WT phenotypes. In each training trial, mice were released from a different starting position, and then were allowed to search for the escape platform for 60 seconds. The platform was submerged 1 cm under the surface of the water. Once a mouse found the platform, it was left there for 15 seconds. If a mouse did not find the platform within 60 seconds, it was guided to the platform and allowed to remain on the platform for 15 seconds before being removed from the pool. Memory was assessed in probe trials that were given after completion of training. During the probe trials, the platform was removed and the mice were allowed to search for it for 60 seconds. Data were acquired and analysed using WaterMaze software (Actimetrics, Wilmette, Illinois, USA).

Social recognition—The social recognition task included training and test sessions. Before training, mice were handled 2 min per day for 3 days, and then habituated to an experimental box for 10 min for another 2 days. During the 10 min training session, mice were allowed to explore the box for 5 min. Then they were exposed and interacted with an ovariectomized (OV) female mouse (3–6 month old, 129/SvJ – #000691 – purchased from Jackson Lab) that was placed under a wired cylinder for another 5 min. During the test session (24 h after training), mice were placed back into the experimental box and allowed to interact with two OV females one familiar and one novel.

Analyses of the behavioural data—For social recognition performance, we compared the time spent with a novel vs. a familiar mouse, for WT and $Nf1^{+/-}$ mice, (paired sample Student's *t*-tests, significance level of 5%). We also computed a two-way ANOVA to test for an interaction between genotype and social stimulus type. For the water maze probe tests, three parameters were analysed: the time spent in the training quadrant, the number of platform crossings and the proximity to the training platform. For quadrant time, we compared the time the mice spent in the training quadrant vs. the average time they spent in the other three quadrants. For platform crossings, we compared the number of crossings of the site where the training platform was during training vs. the average number of crossings in comparable sites in the other three quadrants. These analyses were implemented through two-way ANOVA tests. We also evaluated the average proximity to the training platform, with independent samples Student's *t*-test.

Correlation between volumetric and behavioural data

We assessed the correlation between brain structure volumes and social recognition performance (fraction of time spent with a novel mice), at a significance level of 5%, followed by FDR correction.

Spatial performance revealed a clustering pattern consistent with variable phenotypic penetrance: a cluster of $Nf1^{+/-}$ mice showing performances similar to WT mice (higher performance cluster), while another cluster of $Nf1^{+/-}$ mice showed considerably reduced performance levels, which were linearly separable (see below) from the higher performance cluster. This justified the calculation of correlations separately for each cluster.

To get an overall measure of spatial learning performance, we first combined the measurements from the spatial learning task into a unique combined index ($Index_C$, eqn 1).

$$\text{Index}_c = \frac{\text{Index}_{\text{QT}} + \text{Index}_{\text{PC}} + \text{Proximity}_N}{3}. \quad (1)$$

The discriminant index for quadrant time (Index_{QT}, eqn 2) and the discriminant index for platform crossings (Index_{PC}, eqn 3) are shown below:

$$\text{Index}_{\text{QT}} = \frac{\text{Time in training quadrant}}{\text{Time in training quadrant} + \text{average time in other quadrants}} \quad (2)$$

$$\text{Index}_{\text{PC}} = \frac{\text{Crossings in training quadrant}}{\text{Crossings in training quadrant} + \text{average crossing in other quadrants}}. \quad (3)$$

The normalised proximity (Proximity_N, eqn 4) was computed as:

$$\text{Proximity}_N = 1 - \frac{\text{Distance}_i - \text{Distance}_{\min}}{\text{Distance}_{\max} - \text{Distance}_{\min}}, \quad (4)$$

where Distance_i is the mean distance to the platform for each mouse, $\text{Distance}_{\max}$ and $\text{Distance}_{\min}$ are the maximum and minimum average distances overall for the $Nf1^{+/-}$ group. Thus, the combined index will have values closer to zero for animals with lower performance, and values closer to one for animals with higher performance.

The combined index was then used to divide the $Nf1^{+/-}$ mice into two groups matched in size (high and low performance mice), and then we submitted it to 3D linear discriminant analysis (LDA) for testing accuracy and precision of this division (Fig. 2). The presence of maximum accuracy and precision encouraged us to proceed with the correlation analysis for each cluster separately.

Results

Volumetric analysis

Significant group differences were found in the PFC, CPu and hippocampus, and volumes were higher for $Nf1^{+/-}$ mice in all these regions (Fig. 3). No volumetric correlation with animal sex (PFC: $P = 0.5359$, $F = 0.4$; CPu: $P = 0.3028$, $F = 1.12$; hip -pocampus: $P = 0.1286$, $F = 2.52$) and no sex–genotype interactions (PFC: $P = 0.1863$, $F = 1.88$; CPu: $P = 0.9829$, $F = 0$; hippocampus: $P = 0.1678$, $F = 2.06$) were found, when analysed by ANOVA.

DTI analysis

From the voxel-based analysis, and using a significance level of 5% followed by FDR correction, we found significant group differences concerning MD maps. MD was higher in

$Nf1^{+/-}$ mice in cortical structures (including the PFC), septum, striatum, globus pallidus, hippocampus, thalamus, PAG and midbrain (Fig. 4). With a voxel-based analysis, no significant differences were found for FA maps.

When assessing the average of diffusivity parameters over the main structures of interest, significant differences were seen for all of them, as presented in Table 2. For all the structures of interest and for all the parameters evaluated, higher diffusivity values were observed in $Nf1^{+/-}$ mice

Moreover, comparisons between right and left hemispheres revealed significantly different MD values in the structures of interest, as shown in the Table 3. No differences were observed for FA maps

Behavioural assessment

We replicated previous findings (Costa *et al.* 2002; Cui *et al.* 2008; Shilyansky *et al.* 2010a, b) of impaired spatial learning performance in $Nf1^{+/-}$ mice. As expected, WT mice but not $Nf1^{+/-}$ mice crossed the site where the platform was during training more often than comparable sites in the other three quadrants (Fig. 5a). Unlike Platform crossings, which require that mice cross the exact site where the platform was during training, quadrant time simply measures the time the mice spent in the quadrant where the platform was during training With this less spatially stringent measure, we found evidence that some $Nf1^{+/-}$ mice acquired some spatial information Although the fraction of time spent in quadrant did not show a genotype × place interaction, the average time the WT mice spent in the training quadrant compared to the other three quadrants is significantly higher, while analysis of the performance of $Nf1^{+/-}$ mice showed similar searching time in the target quadrant vs. other quadrants (Fig. 5b).

However, as previously reported, their performance is not uniform (Silva *et al.* 1997) and LDA of spatial performance identified at least two clusters (see below). Finally, average proximity was significantly different between the WT and the $Nf1^{+/-}$ mice used for MRI analysis (Fig. 5c).

In the platform crossing measure during probe trials, $Nf1^{+/-}$ mutants crossed the training platform site significantly less frequently than WT mice (this is a more sensitive measure than latency, see Figures S2 and S3; two-way anova, $P = 0.0156$, $F_{126} = 6.693$; multiple comparison: WT, n=13, $P = 0.0004$; $Nf1^{+/-}$, $n = 15$, $P = 0.6117$). In % time spend in quadrant, WT mice showed significantly higher searching time in target quadrant than other quadrants; $Nf1^{+/-}$ mutants showed similar searching time in target quadrant vs. other quadrants (Figure S4; two-way anova, $P = 0.1317$ $F_{1,26} = 2.422$; multiple comparison: WT, n=13, $P = 0.0006$; $Nf1^{+/-}$, $n = 15$, $P = 0.0683$).

Previous studies had shown that $Nf1^{+/-}$ mice display mild deficits in water maze task in comparison to WT mice. In this experiment, we used three common measures to quantify learning. Two of the measures, platform crossing and proximity, showed significant genotype-related interaction between WT and $NF1^{+/-}$. The other measure, % of time spent in quadrant, did not show genotypes × place interaction. Nevertheless, a planned comparison

showed that WT mice exhibit significant learning (more time in platform quadrant than other quadrants) while $NF1^{+/-}$ mice do not, as previous studies showed. All together, these results demonstrate that that $NF1^{+/-}$ display learning deficits in water maze task.

From the test for social cognition assessment, we found that unlike WT mice, which spent significantly more time with the novel mouse, $Nf1^{+/-}$ mice did not discriminate between novel and familiar mice (Fig. 5d), a result that confirms their social cognition deficits (Molosh *et al.* 2014). A two-way ANOVA also suggested an interaction between genotype and type of social stimulus ($F = 3.57$, $P = 0.06$) although at a marginal significance level.

Correlation between volumetric and behavioural data

We found a significant correlation between PFC volumes in the $Nf1^{+/-}$ group and social discrimination performance as measured by the fraction of time spent with novel mice ($P = 0.0206$; $r = -0.601$; Fig. 6) and this correlation survived to FDR corrections. In contrast, no such correlation was found for the WT mice ($P = 0.853$, $r = -0.0787$; Fig. 6). Although the nature of this analysis is not causal, it agrees with the notion that the PFC has a critical role in social functioning (Adolphs 2009).

Analyses of spatial learning in the $Nf1^{+/-}$ group with lower performance uncovered a significant correlation between the $Index_{QT}$ and CPu volumes ($P = 0.0447$; $r = 0.7658$). We did not found significant correlation between parameters related to spatial learning and the other investigated structures (i.e. PFC and hippocampus). Despite the correlational nature of observations, they are in line with the notion of a dampened contribution to learning.

Discussion

In this study, featuring a structure–function correlation approach, we found indications for an important role of the PFC in the social cognition deficits in the $Nf1^{+/-}$ mouse model. The PFC and CPu were chosen as regions of interest for analyses because previous human studies had already shown impairments in these structures (Cutting *et al.* 2002; Duarte *et al.* 2014; Greenwood *et al.* 2005; Karlsgodt *et al.* 2012; Loitfelder *et al.* 2015; Shilyansky *et al.* 2010a, b; Steen *et al.* 2001; Violante *et al.* 2013). Despite their correlational (non-causal) nature, these results are interesting because they point to an important role of high-level structures such as the PFC in social cognition, in addition to the amygdala (Molosh *et al.* 2014).

Our studies also suggest that compensatory mechanisms in the CPu may be associated with spatial learning impairments in underperforming $Nf1^{+/-}$ mice. Although not the main focus of this article, these results are relevant because of the known interaction, often of competitive nature, between the hippocampus and basal ganglia structures during learning (Poldrack & Rodriguez 2004).

The volumetric analyses developed in this study, revealed higher volumes in key brain regions of interest in $Nf1^{+/-}$ mice, including the PFC, CPu and hippocampus. These results are largely consistent with structural studies in NF1 patients, where increases in white matter (WM) and GM volumes were frequently observed (Duarte *et al.* 2014; Karlsgodt *et al.* 2012;

Margariti *et al.* 2007; Pride *et al.* 2014), as opposed to GM reductions in a few other regions (Cutting *et al.* 2002; Duarte *et al.* 2014; Pride *et al.* 2014; see also, Table 1).

Concerning brain diffusivity we found a widespread, beyond our regions of interest, cortical and subcortical increase in MD, as shown from MD maps, which is also consistent with studies in NF1 patients (Filippi *et al.* 2013; Santos 2011; Table 1). Importantly, the average diffusivities over the structures of interest also showed increases on MD and FA, due to increases in both RD and $\lambda 1$. No major axonal disorganization or disruption seems to be present in $Nf1^{+/-}$ mice brains, and the MD and FA differences could be a consequence of increased spacing between axons. This notion is also consistent with a study in NF1 patients by Violante *et al.* (2013). Moreover, inter-hemispheric differences in MD were also observed, which a pattern often found in neurodevelopmental disorders due to their slightly distinct developmental trajectory (Table 3).

The PFC, CPu and hippocampus showed differences in both volumetric and DTI analyses. These brain structures are known to be involved in a wide range of cognitive functions. Concerning the hippocampus, a clear relationship has been previously established with impairments in spatial learning and working memory which have been related to abnormalities in gabaergic mediated inhibition identified in the hippocampus (Costa *et al.* 2002; Cui *et al.* 2008). These seem to also be present in the PFC and CPu (Shilyansky *et al.* 2010a,b).

Social discrimination deficits had been previously recognized in $Nf1^{+/-}$ mice (Molosh *et al.* 2014). Compared to WT mice, the $Nf1^{+/-}$ mice showed reduced preference for novel conspecifics during a social memory test given 24 h after the initial social interaction. These findings are consistent with evidence in human behavioural and structural studies indicating that NF1 patients have social cognition impairments consistent with the autistic spectrum (Lehtonen *et al.* 2013; Plasschaert *et al.* 2015; Pride *et al.* 2013, 2014; Walsh *et al.* 2013). Importantly, a significant linear correlation was observed between PFC volumes and social discrimination ability in the $Nf1^{+/-}$ group, as measured by the fraction of time spent with novel mice. This result does not allow for causal inference but supports the hypothesis that in addition to the amygdala (Molosh *et al.* 2014), alterations in PFC in $Nf1^{+/-}$ mice (and also in NF1 patients) contribute to the social deficits of these mice. This finding is consistent with a recent human study in NF1 patients, suggesting an important role for the frontal cortex in social cognition performance (Loitfelder *et al.* 2015).

Interestingly, a significant correlation was observed between the $Index_{QT}$ and CPu volumes in underperforming $Nf1^{+/-}$ mice. CPu volumes were also found to be increased in NF1 patients (Violante *et al.* 2013). This finding is consistent with that of striatal networks being largely prone to functional reorganization (Poldrack & Rodriguez 2004).

The findings reported here suggest an avenue for future research. For example, some of the authors have previously observed that lovastatin reverses the behavioural phenotype of $Nf1^{+/-}$ mice (Li *et al.* 2005). It remains an outstanding question whether structural and neurochemical impairments could be reversed. Nevertheless, the former might only be partially reversible, given the nature of neural proliferation during development.

To conclude, in this structure–function phenotyping study, we found evidence that suggests a role for the PFC and the CPu in the social cognition deficits found in the $Nf1^{+/-}$ mouse model. Importantly, changed PFC volumes were related to social deficits observed in $Nf1^{+/-}$ mice. The structural and functional findings reported here may be relevant for longitudinal studies of cognitive function in NF1, and they may also instruct current and future efforts to find a treatment for cognitive and social deficits in this population.

Supplementary Material

Refer to Web version on PubMed Central for supplementary material.

Acknowledgments

This work was supported by MH084315 to A.J.S. and CENTRO-07-ST24-FEDER-00205, PTDC/SAU-ORG/118380/2010, Grant FCT UID/NEU/04539/2013-2020, COMPETE, POCI-01-0145-FEDER-007440 to M.C.B. and FCT fellowship SFRH/BPD/ 112863/2015 to L.I.P.

References

Adolphs R. The social brain: neural basis of social knowledge. Annu Rev Psychol. 2009; 60:693–716. DOI: 10.1146/annurev.psych.60.110707.163514 [PubMed: 18771388]

Balestri P, Vivarelli R, Grosso S, Santori L, Farnetani MA, Galluzzi P, Vatti GP, Calabrese F, Morgese G. Malformations of cortical development in neurofibromatosis type 1. Neurology. 2003; 61:1799–1801. [PubMed: 14694053]

Costa RM, Silva AJ. Mouse models of neuro bromatosis type I: bridging the GAP. Trends Mol Med. 2003; 9:19–23. [PubMed: 12524206]

Costa RM, Federov NB, Kogan JH, Murphy GG, Stern J, Ohno M, Kucherlapati R, Jacks T, Silva AJ. Mechanism for the learning deficits in a mouse model of neurofibromatosis type 1. Nature. 2002; 415:526–530. DOI: 10.1038/nature711 [PubMed: 11793011]

Cui Y, Costa RM, Murphy GG, Elgersma Y, Zhu Y, Gutmann DH, Parada LF, Mody I, Silva AJ. Neurofibromin regulation of ERK signaling modulates GABA release and learning. Cell. 2008; 135:549–560. DOI: 10.1016/j.cell.2008.09.060.Neurofibromin [PubMed: 18984165]

Cutting LE, Koth CW, Burnette CP, Abrams MT, Kaufmann WE, Bridge Denckla M. Relationship of cognitive functioning, whole brain volumes, and T2-weighted hyperintensities in neurofibromatosis-1. J Child Neurol. 2000; 15:157–160. DOI: 10.1177/088307380001500303 [PubMed: 10757470]

Cutting LE, Cooper KL, Koth CW, Mostofsky SH, Kates WR, Denckla MB, Kaufmann WE. Megalencephaly in NF1: predominantly white matter contribution and mitigation by ADHD. Neurology. 2002; 59:1388–1394. DOI: 10.1212/01.WNL.0000032370.68306.8A [PubMed: 12427889]

Diggs-Andrews KA, Gutmann DH. Modeling cognitive dysfunction in neurofibromatosis-1. Trends Neurosci. 2013; 36:237–247. DOI: 10.1016/j.tins.2012.12.002 [PubMed: 23312374]

Duarte JV, Ribeiro MJ, Violante IR, Cunha G, Silva E, Castelo-Branco M. Multivariate pattern analysis reveals subtle brain anomalies relevant to the cognitive phenotype in neurofibromatosis type 1. Hum Brain Mapp. 2014; 35:89–106. DOI: 10.1002/hbm.22161 [PubMed: 22965669]

Filippi CG, Watts R, Duy LAN, Cauley KA. Diffusion-tensor imaging derived metrics of the corpus callosum in children with neurofibromatosis type I. Am J Roentgenol. 2013; 200:44–49. DOI: 10.2214/AJR.12.9590 [PubMed: 23255740]

Fischl B, Salat DH, Busa E, Albert M, Dieterich M, Haselgrove C, Van Der Kouwe A, Killiany R, Kennedy D, Klaveness S, Montillo A, Makris N, Rosen B, Dale AM. Whole brain segmentation: automated labeling of neuroanatomical structures in the human brain. Neuron. 2002; 33:341–355. DOI: 10.1016/S0896-6273(02)00569-X [PubMed: 11832223]

Greenwood RS, Tupler LA, Whitt JK, Buu A, Dombeck CB, Harp AG, Payne ME, Eastwood JD, Krishnan KRR, Mac-Fall JR. Brain morphometry, T2-weighted hyperintensities, and IQ in children with neurofibromatosis type 1. Arch Neurol. 2005; 62:1904–1908. DOI: 10.1001/archneur.62.12.1904 [PubMed: 16344348]

Gutmann DH, Wu YL, Hedrick NM, Zhu Y, Guha A, Parada LF. Heterozygosity for the neurofibromatosis 1 (NF1) tumor suppressor results in abnormalities in cell attachment, spreading and motility in astrocytes. Hum Mol Genet. 2001; 10:3009–3016. DOI: 10.1093/hmg/10.26.3009 [PubMed: 11751683]

Karlsgodt KH, Rosser T, Lutkenhoff ES, Cannon TD, Silva AJ, Bearden CE. Alterations in white matter microstructure in neurofibromatosis-1. PLoS One. 2012; 7:1–11. DOI: 10.1371/journal.pone.0047854

Lehtonen A, Howie E, Trump D, Huson SM. Behaviour in children with neurofibromatosis type 1: cognition, executive function, attention, emotion, and social competence. Dev Med Child Neurol. 2013; 55:111–125. doi:10. 1111/j.1469-8749.2012.04399.x. [PubMed: 22934576]

Li W, Cui Y, Kushner SA, Brown RAM, Jentsch JD, Frankland PW, Cannon TD, Silva AJ. The HMG-CoA reductase inhibitor lovastatin reverses the learning and attention deficits in a mouse model of neurofibromatosis type 1. Curr Biol. 2005; 15:1961–1967. DOI: 10.1016/j.cub.2005.09.043 [PubMed: 16271875]

Loitfelder M, Huijbregts SCJ, Veer IM, Swaab HS, Van Buchem MA, Schmidt R, Rombouts SA. Functional connectivity changes and executive and social problems in neurofi-bromatosis type I. Brain Connect. 2015; 5:312–320. DOI: 10.1089/brain.2014.0334 [PubMed: 25705926]

Mainberger F, Jung NH, Zenker M, Wahlländer U, Freudenberg L, Langer S, Berweck S, Winkler T, Straube A, Heinen F, Granström S, Mautner VF, Lidzba K, Mall V. Lovas-tatin improves impaired synaptic plasticity and phasic alertness in patients with neurofibromatosis type 1. BMC Neurol. 2013; 13:131–142. DOI: 10.1186/1471-2377-13-131 [PubMed: 24088225]

Margariti PN, Blekas K, Katzioti FG, Zikou AK, Tzoufi M, Argyropoulou MI. Magnetization transfer ratio and volumetric analysis of the brain in macrocephalic patients with neurofibromatosis type 1. Eur Radiol. 2007; 17:433–438. DOI: 10.1007/s00330-006-0323-1 [PubMed: 16733674]

Molosh AI, Johnson PL, Spence JP, Arendt D, Federici LM, Bernabe C, Janasik SP, Segu ZM, Khanna R, Goswami C, Zhu W, Park SJ, Li L, Mechref YS, Clapp DW, Shekhar A. Social learning and amygdala disruptions in Nf1 mice are rescued by blocking p21-activated kinase. Nat Neurosci. 2014; 17:1583–1590. DOI: 10.1038/nn.3822 [PubMed: 25242307]

Moore BD, Slopis JM, Jackson EF, De Winter AE, Leeds NE. Brain volume in children with neurofibromatosis type 1: relation to neuropsychological status. Neurology. 2000; 54:914–920. DOI: 10.1212/WNL.54.4.914 [PubMed: 10690986]

Plasschaert E, Descheemaeker MJ, Van Eylen L, Noens I, Steyaert J, Legius E. Prevalence of autism spectrum disorder symptoms in children with neurofibromatosis type 1. Am J Med Genet B Neuropsychiatr Genet. 2015; 168B:72–80. DOI: 10.1002/ajmg.b.32280 [PubMed: 25388972]

Poldrack RA, Rodriguez P. How do memory systems interact? Evidence from human classification learning. Neurobiol Learn Mem. 2004; 82:324–332. DOI: 10.1016/j.nlm.2004.05.003 [PubMed: 15464413]

Pride NA, Crawford H, Payne JM, North KN. Social functioning in adults with neurofibromatosis type 1. Res Dev Disabil. 2013; 34:3393–3399. DOI: 10.1016/j.ridd.2013.07.011 [PubMed: 23911645]

Pride NA, Korgaonkar MS, Barton B, Payne JM, Vucic S, North KN. The genetic and neuroanatomical basis of social dysfunction: lessons from neurofibromatosis type 1. Hum Brain Mapp. 2014; 35:2372–2382. DOI: 10.1002/hbm.22334 [PubMed: 23881898]

Ribeiro MJ, Violante IR, Bernardino I, Ramos F, Saraiva J, Reviriego P, Upadhyaya M, Silva ED, Castelo-Branco M. Abnormal achromatic and chromatic contrast sensitivity in neurofibromatosis type 1. Invest Ophthalmol Vis Sci. 2012; 53:287–293. DOI: 10.1167/iovs.11-8225 [PubMed: 22190595]

Rizvi TA, Akunuru S, Courten-Myers G, Switzer RC, Nordlund ML, Ratner N. Region-specific astrogliosis in brains of mice heterozygous for mutations in the neurofibromatosis type 1 (Nf1) tumor suppressor. Brain Res. 1999; 816:111–123. DOI: 10.1016/S0006-8993(98)01133-0 [PubMed: 9878702]

Robinson A, Kloog Y, Stein R, Assaf Y. Motor deficits and neurofibromatosis type 1 (NF1)-associated MRI impairments in a mouse model of NF1. NMR Biomed. 2010; 23:1173–1180. DOI: 10.1002/nbm.1546 [PubMed: 20586111]

Rosenbaum T, Engelbrecht V, Krölls W, Van Dorsten FA, Hoehn-Berlage M, Lenard HG. MRI abnormalities in neurofibromatosis type 1 (NF1): a study of men and mice. Brain Dev. 1999; 21:268–273. DOI: 10.1016/S0387-7604(99)00024-8 [PubMed: 10392751]

Santos, A. Fac Sci Technol Univ Coimbra. University of Coimbra; 2011. Visual-callosal white matter pathways in neurofi-bromatosis type 1: a Diffusion Tensor Imaging – Fiber Tracking (DTI-FT) study.

Shilyansky C, Karlsgodt KH, Cummings DM, Sidiropoulou K, Hardt M, James AS, Ehninger D, Bearden CE, Poirazi P, Jentsch JD, Cannon TD, Levine MS, Silva AJ. Neurofibromin regulates corticostriatal inhibitory networks during working memory performance. Proc Natl Acad Sci USA. 2010a; 107:13141–13146. DOI: 10.1073/pnas.1004829107 [PubMed: 20624961]

Shilyansky C, Lee YS, Silva AJ. Molecular and cellular mechanisms of learning disabilities: a focus on NF1. Annu Rev Neurosci. 2010b; 33:221–243. DOI: 10.1146/annurev-neuro-060909-153215 [PubMed: 20345245]

Silva AJ, Frankland PW, Marowitz Z, Friedman E, Laszlo GS, Cioffi D, Jacks T, Bourtchuladze R. A mouse model for the learning and memory deficits associated with neurofibromatosis type I. Nat Genet. 1997; 15:281–284. DOI: 10.1038/ng0397-281 [PubMed: 9054942]

Steen RG, Taylor JS, Langston JW, Glass JO, Brewer VR, Reddick WE, Mages R, Pivnick EK. Prospective evaluation of the brain in asymptomatic children with neurofibromatosis type 1: relationship of macrocephaly to T1 relaxation changes and structural brain abnormalities. AJNR Am J Neuroradiol. 2001; 22:810–817. [PubMed: 11337320]

Theos A, Korf BR. Pathophysiology of neurofibromatosis type 1. Ann Intern Med. 2006; 144:842–849. [PubMed: 16754926]

van der Vaart T, van Woerden GM, Elgersma Y, de Zeeuw CI, Schonewille M. Motor deficits in neurofibromatosis type 1 mice: the role of the cerebellum. Genes Brain Behav. 2011; 10:404–409. doi:101111/j1601-183X.201100685.x. [PubMed: 21352477]

Violante IR, Ribeiro MJ, Silva ED, Castelo-Branco M. Gyrification, cortical and subcortical morphometry in neurofibromatosis type 1: an uneven profile of developmental abnormalities. J Neurodev Disord. 2013; 5:1–13. DOI: 10.1186/1866-1955-5-3 [PubMed: 23402354]

Walsh KS, Vélez JI, Kardel PG, Imas DM, Muenke M, Packer RJ, Castellanos FX, Acosta MT. Symptomatology of autism spectrum disorder in a population with neurofibromatosis type 1. Dev Med Child Neurol. 2013; 55:131–138. doi:101111/dmcn.12038. [PubMed: 23163951]

Wignall EL, Griffiths PD, Papadakis NG, Wilkinson ID, Wallis LI, Bandmann O, Cowell PEE, Hoggard N. Corpus callosum morphology and microstructure assessed using structural MR imaging and diffusion tensor imaging: initial findings in adults with neurofibromatosis type 1. AJNR Am J Neuroradiol. 2010; 31:856–861. DOI: 10.3174/ajnr.A2005 [PubMed: 20299428]

Zamboni SL, Loenneker T, Boltshauser E, Martin E, Il'yasov KA. Contribution of diffusion tensor MR imaging in detecting cerebral microstructural changes in adults with neurofibromatosis type 1. AJNR Am J Neuroradiol. 2007; 28:773–776. doi:28/4/773[pii]. [PubMed: 17416837]

Zöller ME, Rembeck B, Bäckman L. Neuropsychologica deficits in adults with neurofibromatosis type 1. Acta Neurol Scand. 1997; 95:225–232. [PubMed: 9150813]

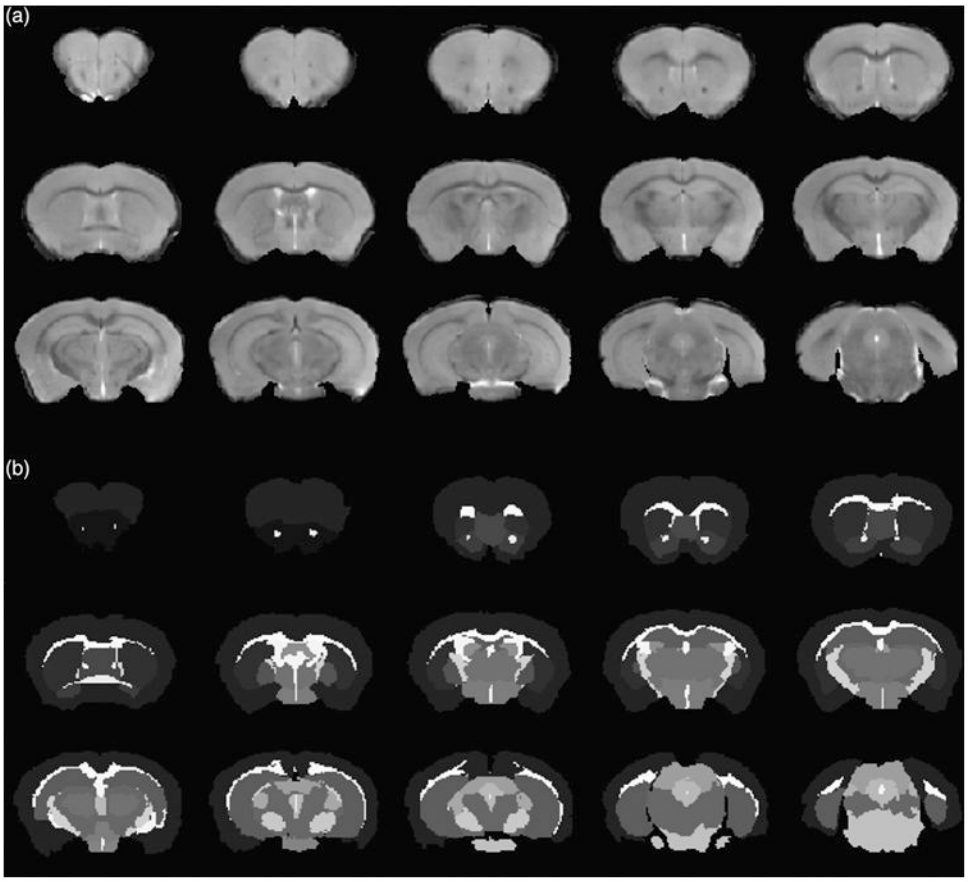

Figure 1.
(a) Anatomical (T2-weighted) images and (b) the resulting segmentation, from a subset of slices including PFC, CPu and the hippocampus.

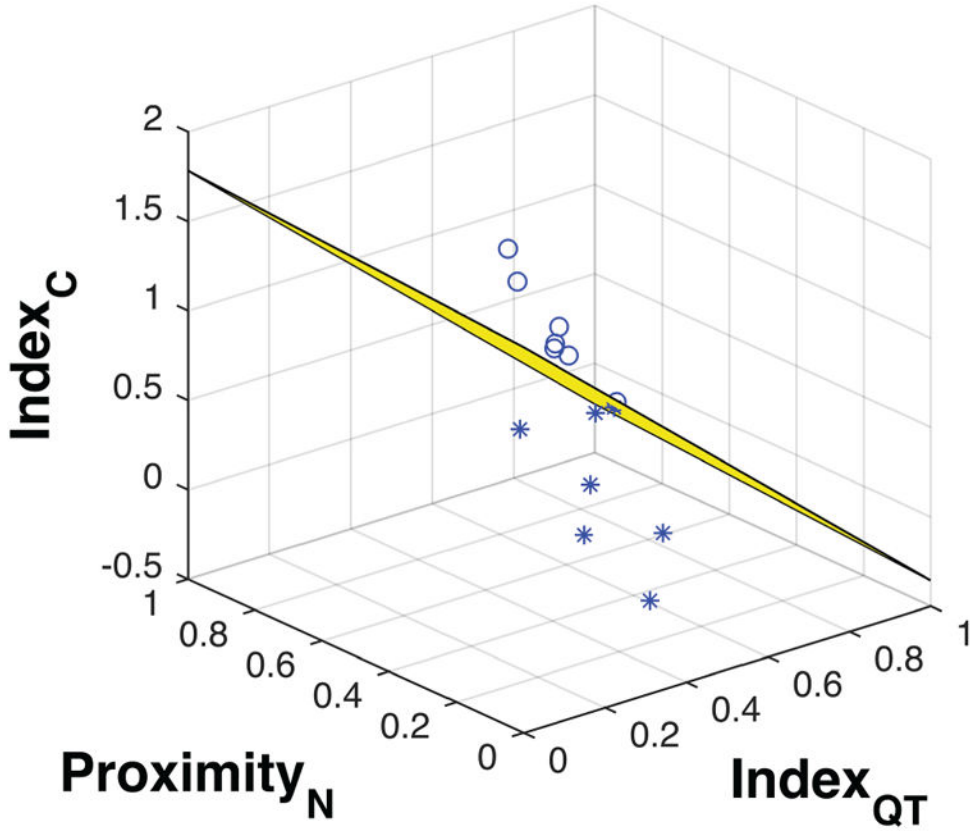

Figure 2. Result from LDA (with maximum accuracy and precision) on dividing Nf1$^{+/-}$ mice in two groups based on water maze test performance

Spherical and star markers represent the high and low performance groups, respectively.

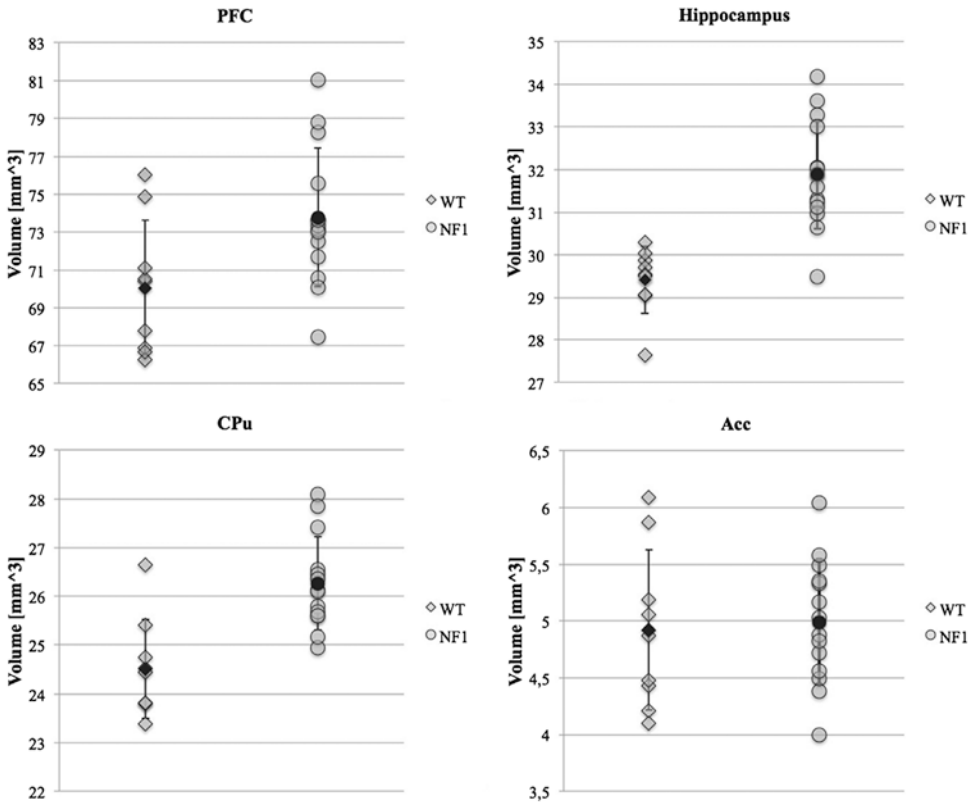

Figure 3. Volume measurements for WT and Nf1$^{+/-}$ mice on: PFC (*P* = 0.0268, *t* = −2.42, df = 17), hippocampus (*P* <0.0001, *t* = −5.77, df = 21), CPu (*P* = 0.0007, *t* = −4.16, df = 16) and accumbens (*P* = 0.8139, *t* = −0.24, df = 14)

Statistical results were obtained from independent samples *t*-test. Mean values (black shapes) and standard deviation bars are represented.

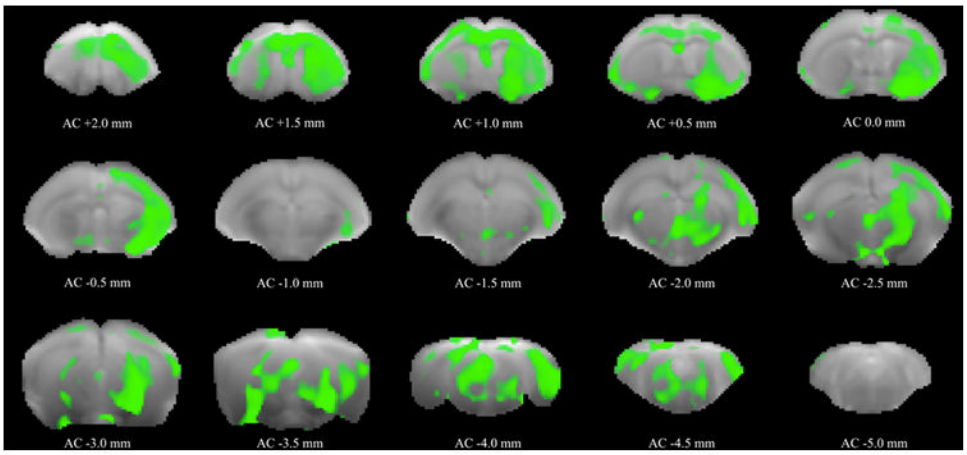

Figure 4. Regions with significant statistical differences (green) concerning MD maps distributed along the cortex, striatum, globus pallidus, thalamus, hippocampus, midbrain and PAG

The results were obtained from independent samples *t*-tests with 5% of significance level, followed by FDR correction ($Q = 5\%$). In the figure, statistical data are superimposed to b0 images, and the plane positions are indicated with reference to the anterior commissure (AC).

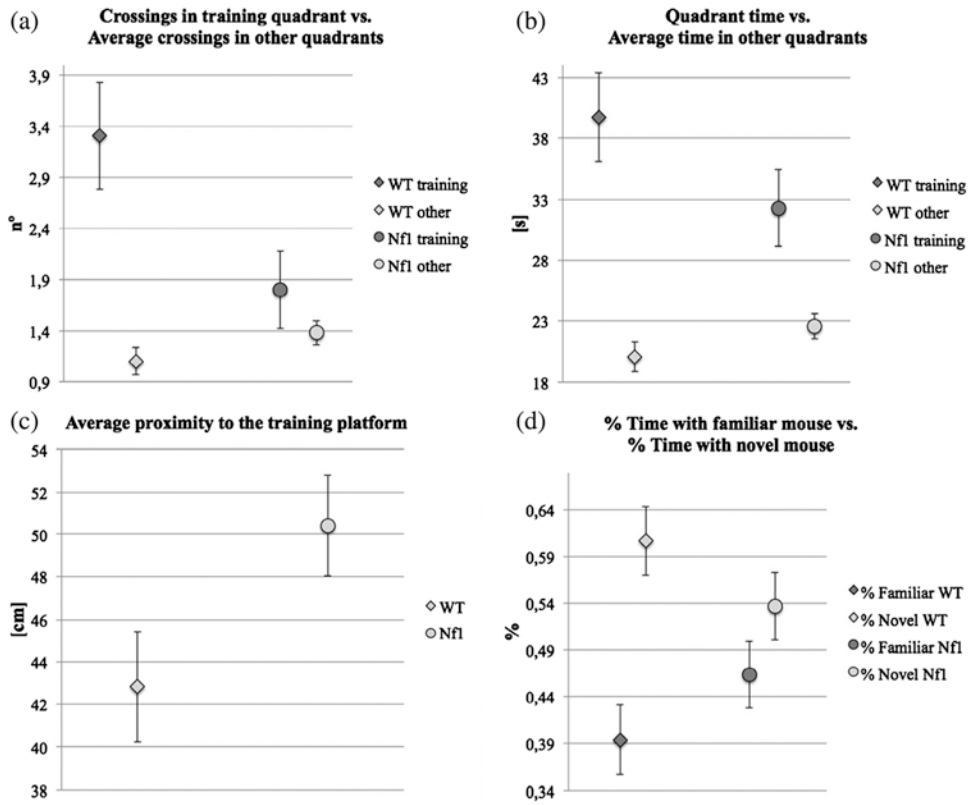

Figure 5. Results from the water maze and social recognition tests (mean values and standard deviation)

(a) Platform crossings vs. average crossings in other quadrants, two-way ANOVA, $P = 0.0156$, $F_{1,26} = 6.693$; multiple comparisons: WT $P = 0.0004$ and Nf1$^{+/-}$ $P = 0.6117$. (b) Time in training quadrant vs. average time in other quadrants, two-way ANOVA, $P = 0.1317$, $F_{1,26} = 2.422$; multiple comparison: WT $P = 0.0006$ and Nf1$^{+/-}$ $P = 0.0683$. (c) Average proximity, for WT vs. Nf1$^{+/-}$ mice ($P = 0.0448$, $t = -2.15$, df = 19). (d) Fractions of time with familiar mouse vs. fraction of time with novel mouse, for WT ($P = 0.0156$, $t = -2.85$, df = 11) and Nf1$^{+/-}$ ($P = 0.3328$, $t = -1.01$, d f = 13) mice; two-way ANOVA, interaction term $P = 0.06$, $F = 3.57$.

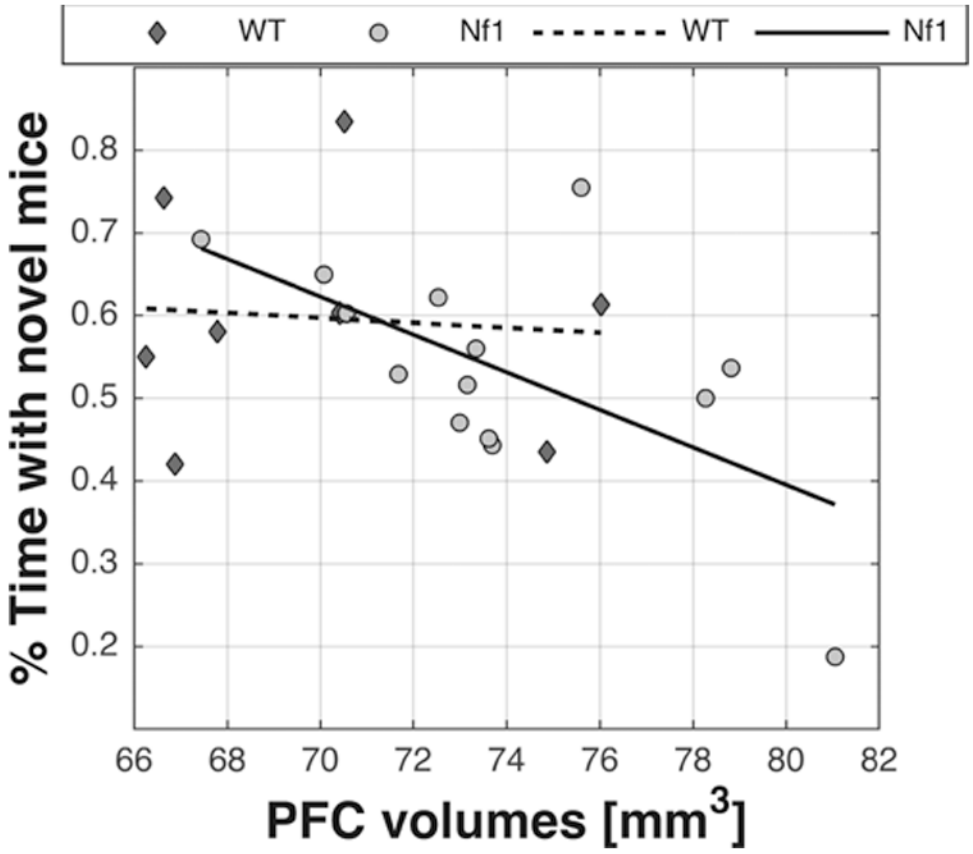

Figure 6.

Linear correlation between PFC volumes and % time with novel mice: WT (diamond markers; $r = -0.0787$; $P = 0.853$) and $Nf1^{+/-}$ mice (round markers; $r = -0.601$; $P = 0.0206$).

Table 1

Summary of human MRI/DTI studies in NF1 (ADC, apparent diffusion coefficient; $\lambda 1$, longitudinal diffusivity; $\lambda 2$ and $\lambda 3$, transverse diffusivity)

Authors	WM volume	GM volume	Brain volume	ADC	MD	FA	RD	$\lambda 2$, $\lambda 3$	$\lambda 1$
Cutting *et al.* (2000)			H						
Moore *et al.* (2000)	H*	H	H						
Steen *et al.* (2001)	H	ND	H						
Cutting *et al.* (2002)	H	H/L	H						
Greenwood *et al.* (2005)	H	H	H						
Margariti *et al.* (2007)	H	H							
Zamboni *et al.* (2007)				H		L			
Wignall *et al.* (2010)	H*		H			L*		H*	ND*
Santos (2011)					H*	L*		H*	ND*
Filippi *et al.* (2013)			ND		H	L†	H†		ND†
Karlsgodt *et al.* (2012)	H	H		H		L	H		H
Duarte *et al.* (2014)	H	H/L							
Pride *et al.* (2014)	ND	H/L	H						

H, higher values in NF1 patients compared to control subjects; L, lower values in NF1 patients compared to control subjects; H/L, H and L were obtained for different brain regions; ND, no differences between NF1 patients and control subjects.

*Observations restricted to visual-callosal WM pathways.

†Observations restricted to the corpus callosum.

Table 2

Average diffusivity parameters over PFC, CPu and hippocampus, and the respective statistical analysis

	MD		FA		λ1		RD	
	WT	Nf1	WT	Nf1	WT	Nf1	WT	Nf1
PFC	6.59e-4 ± 1.85e-5	7.05e-4 ± 2.97e-5	0.0919 ± 0.0196	0.1244 ± 0.0449	7.2e-4 ± 2.62e-5	7.97e-4 ± 5.02e-5	6.28e-4 ± 1.73e-5	6.59e-4 ± 2.58e-5
P values	1.53e-4		0.0096		1.12e-4		0.0023	
t	−4.61		−2.85		−4.77		−3,47	
df	21		21		20		21	
CPu	6.09e-4 ± 1.71e-5	6.55e-4 ± 3.44e-5	0.0903 ± 0.0281	0.128 ± 0.0382	6.65e-4 ± 3.08e-5	7.44e-4 ± 5.66e-5	5.81e-4 ± 1.37e-5	6.11e-4 ± 2.84e-5
P values	3.77e-4		0.013		3.28e-4		0.003	
t	−4.26		−2.72		−4.3		−3.37	
df	20		20		21		20	
Hippocamp	us 6.61e-4 ± 2.31e-5	7.04e-4 ± 3.37e-5	0.0928 ± 0.0269	0.123 ± 0.0327	7.24e-4 ± 4.27e-5	7.93e-4 ± 5.07e-5	6.3e-4 ± 1.55e-5	6.6e-4 ± 2.98e-5
P values	0.0014		0.0259		0.0022		0.0042	
t	−3.67		−2.41		−3.53		−3.22	
df	21		20		19		20	

Table 3

Comparison of MD values between right and left hemispheres in the PFC, CPu and hippocampus

		PFC	CPu	Hippocampus
WT	*P* values	0.4825	0.1592	0.0082
	t	−0.74	1.55	3.49
	df	8	8	8
$Nf1^{+/-}$	*P* values	0.015 7	0.0083	0.00005
	t	−2.78	3.11	5.95
	df	13	13	13